AIAA 93-0901
On the Interaction of a Dense Spray Diffusion Flame and a Potential Vortex

Sheau-Ming Shiah
Chung-Cheng Institute of Technology
Tao-Yuan, Taiwan
and
Martin Sichel
University of Michigan
Ann Arbor, MI

31st Aerospace Sciences Meeting & Exhibit
January 11-14, 1993 / Reno, NV

AIAA-93-0901

ON THE INTERACTION OF A DENSE SPRAY DIFFUSION FLAME AND A POTENTIAL VORTEX

+Sheau-Ming Shiah and *Martin Sichel†

*Aeronautical Engineering Department
Chung-Cheng Institute of Technology
Tao-Yuan, Taiwan 33508
The Republic of China

+Aerospace Engineering Department
The University of Michigan
Ann Arbor Michigan 48109

ABSTRACT

The interaction of a dense spray diffusion flame with a non-decaying potential vortex has been investigated theoretically. A similarity solution for the local structure of the diffusion flamelet in the vortex field has been determined. The global diffusion flame contour generated by the vortex has been determined by patching the flamelet solutions at different distances from the vortex center together. The initially plane spray is assumed to be sufficiently dense so that burning occurs in the sheath combustion mode. The local flamelet analysis shows that with respect to an inertial coordinate frame the spray flamelet moves into the gaseous oxidizer, away from the spray while the edge of the spray moves in the opposite direction with a much smaller velocity. The flamelet motion depends on the properties of the spray and the bounding oxidizer. The local diffusion layer structure of the flame is found to be self similar in terms of the parameter $\Gamma t/2\pi r^2$. The global flame contour is shown to be governed by the circulation diffusivity ratio $\Gamma/2\pi D$. The flame contour is found to bound a spray engulfment and reacted core region near the vortex center where combustion is no longer possible. The radius of this core, which contains reaction products and unburned spray, is found to be proportional to $(\Gamma/2\pi D)^{1/3}$. The augmentation of fuel consumption due to the vortex spray has been calculated and is shown to be independent of time and proportional to $(\Gamma/2\pi D)^{2/3}$. The present results, based on a potential vortex are found to be a good approximation to those for a viscous vortex with the same value of $\Gamma/2\pi D$ as long as this parameter is sufficiently large. While many approximations have been made in this analysis, some of the key parameters governing spray flame vortex interaction have been identified.

INTRODUCTION

The interaction between a diffusion flame and a vortex has recently been studied extensively by many investigators[1-8]. The flame/vortex interaction problem is of great interest due to its relevance to the theoretical study of turbulent diffusion flames. According to Marble[1], who first studied this problem, the flame/vortex interaction can be resolved into a local flamelet analysis and based on these local results the global property of the interaction field can then be established with relative simplicity. Two simplifying features of the original Marble problem are that the density is assumed constant, and that the fuel and oxidizer placed in the vortex field are in stoichiometric proportions, for then the resultant diffusion flame does not move relative to the fluid so that its contour can be determined using vortex kinematics only. However, if the fuel and oxidizer are not in stoichiometric proportions or if the gaseous fuel is replaced by a dense liquid fuel spray, there will be relative motion between the diffusion flame and the vortex. In these situations the resultant flame contour can no longer be determined using only vortex kinematics; it becomes necessary to take into account the local flamelet motion, complicating the analysis of the original Marble problem.

In a previous paper of the present authors[8], the effect of flame motion was resolved; however, a non-decaying potential vortex rather than a viscous vortex was considered in order to simplify the analysis. The results showed that flamelet motion, governed by the *background* equivalence ratio ϕ for the diffusion flame, will occur such that flamelets move toward the oxidizer for $\phi > 1$, and toward the fuel, for $\phi < 1$. A patching method was then developed for computing contours of these non-stationary flames, and the flame contours thus obtained were shown to be similar to the numerical results reported by Laverdant and Candel[4], thus justifying the applicability of the patching method. It should be noted that the background equivalence ratio ϕ as used here refers to the initial concentration of the fuel and oxidizer on the two sides of the diffusion flame sheet.

The present paper is a continuation of this study[8] and considers the interaction of a planar spray diffusion flame with a potential non-decaying vortex. The focus is placed on the flame contour, the size of the reacted region, and the augmentation in global fuel consumption rate. The spray consists of saturated fuel droplets with a large heat of vaporization and inert gas and is assumed sufficiently dense so that combustion of the spray is governed by the sheath combustion mode described by Sichel and Palaniswamy[9]. Then the resultant flame will be external to the spray and vaporization of the spray is confined to a thin sheath or inwardly propagating vaporizing wave at the edge of the spray while the spray interior is unaffected and remains cool and saturated. The spray flamelet analysis is based on the assumptions of constant density and transport coefficients, the Burke-Schumann flame sheet approximation, and the locally one-dimensional approximation used by Marble[1]. The vortex-distorted spray flame contour is constructed by the patching method developed in Ref. 8, for treating the gaseous nonstoichiometric diffusion flame. For interpretation, the case of an octane spray/air diffusion flame is studied for several values of the vortex circulation diffusivity ratio, Γ/D, and of the spray droplet mass fraction, Y_d.

†Professor, Department of Aerospace Engineering
Fellow

LOCAL FLAMELET ANALYSIS

The initial configuration of the present problem is shown in Fig. 1(a), which illustrates a spray diffusion flame at the instant the spray and oxidizer first come into contact and a non-decaying plane potential vortex with the tangential velocity $v_\theta = \Gamma/2\pi r$, at the flame surface. According to Ref. 1, in the absence of flamelet motion a typical contour of the flame, distorted by the vortex motion after some time has elapsed, will appear as shown by the solid curve in Fig. 1(b). However, following Ref. 8 the present spray flamelets will move toward the oxidizer, following the arrowheads while the edge of the spray moves in the opposite direction as indicated by the dot symbols. It is likely that as the flame continues to be wound up by the vortex, the two branches of flame will coalesce in region I.

Local Flamelet Flow

Following Ref. 1, the local configuration of the present problem can be described by a moving spray flamelet in the field of an opposed fuel spray and gaseous oxidizer flow, as shown in Fig. 2. The velocity v_v of the opposed flow generated by the vortex with $v_\theta = \Gamma/2\pi r$ is shown to be: $v_v = \varepsilon y_1$, where the flow strain rate $\varepsilon = -K(\zeta)/t$; $K(\zeta) \equiv 4\zeta^2/(1 + 4\zeta^2)$; and $\zeta \equiv \Gamma t/2\pi r^2$. To include the effect of spray vaporization on the local flow, the configuration shown in the central part of Fig. 2 must be considered. Following Ref. 9, during sheath combustion of a fuel droplet cloud, the cloud edge moves into the cloud with the vaporization wave speed while the vaporized species moves away from the cloud. Here, the wave speed and the vapor velocity are denoted by U and v_c, in the y_1 coordinate system fixed to the initial interface location. For convenience, a cloud edge coordinate y is defined, as indicated in Fig. 2, so that $y = 0$ corresponds to the cloud edge and $y > 0$ represents the gas phase region, where combustion occurs. It can be seen that $y = y_1 + \Delta$, and that the cloud is flowing with velocity U and the vapor flux with $U + v_c$ in this system.

By superposing v_v and v_c, the gas phase velocity v near the spray flamelet can be written as:

$$v = -\frac{K(\zeta)}{t}\left(y - \int_0^t U(\zeta,t)\,dt\right) + U(\zeta,t) + v_c(\zeta,t) \quad (1)$$

while the spray phase velocity v_s is obtained by superposing v_v and U so that:

$$v_s = -\frac{K(\zeta)}{t}\left(y - \int_0^t U(\zeta,t)\,dt\right) + U(\zeta,t) \quad (2)$$

where $U(\zeta,t)$ and $v_c(\zeta,t)$ are used for describing flamelets at different locations along the vortex. As described below, the local flamelet analysis will be based on these flows and the results are patched together to determine contours of the vortex-distorted spray flame.

Similarity Solutions

Based on Fig. 2 and following Williams[10], the one-dimensional conservation equations of species and energy for the spray flamelet can be written as:

$$\rho\frac{\partial Y_j}{\partial t} + \rho v\frac{\partial Y_j}{\partial y} = \rho D\frac{\partial^2 Y_j}{\partial y^2} + \omega_j \quad (j = F,O,P) \quad (3)$$

$$\rho C_p\frac{\partial T}{\partial t} + \rho C_p v\frac{\partial T}{\partial y} = \lambda\frac{\partial^2 T}{\partial y_2} - \sum h^o_j\omega_j \quad (4)$$

where the one-step reaction: $v'_F[F] + v'_O[O] = v''_P[P]$ is adopted to represent the flamelet burning process and v is given by Eq. (1). Symbols are defined in the nomenclature.

Using the Shvab-Zeldovich formulation[10] these equations can be reduced to

$$\frac{\partial \beta_i}{\partial t} + v\frac{\partial \beta_i}{\partial y} = D\frac{\partial^2 \beta_i}{\partial y^2} \quad (5)$$

where $\beta_i \equiv \alpha_i - \alpha_o$ $(i = F,P,T)$ and α are defined as follows:

$$\alpha_T \equiv \frac{C_p W_t(T - T_w)}{q^o};\ \alpha_k \equiv \frac{W_t(Y_k - Y_{kw})}{W_k(v''_k - v'_k)};\ (k = F,O,P) \quad (6)$$

where $q^o\omega = -\sum h^o_j\omega_j$; $\omega \equiv \omega_j W_t/W_j(v''_j - v'_j)$; and $W_t \equiv \sum W_j v'_j = W_j v''_j$.

Eq. (5) can be shown [11] to have the similarity solution $\beta_i(\eta)$ written as:

$$\beta_i(\eta) = \beta_{i\infty}\left[\frac{erf\left(\frac{\eta}{2} - E_c\right) + erf(E_c)}{1 + erf(E_c)}\right] \quad (7)$$

provided that $\eta \equiv C(\zeta)\, y/\sqrt{Dt}$ and

$$v = -K(\zeta)\, y/t + C(\zeta)\, E_c\sqrt{D/t} \quad (8)$$

are satisfied, where $C^2(\zeta) \equiv (3 + 12\zeta^2)/(3 + 4\zeta^2)$ and the parameter E_c represents an eigenvalue of the solution. E_c is determined from flux balance equations at the edge of the spray, as described below.

Regression of the Spray

The spray regression speed $U(\zeta,t)$ can be determined from the equation of mass flux balance at the spray edge, which is written as:

$$\rho C(\zeta)\, E_c\sqrt{D/t} = \rho_c U_s(\zeta,t) \quad (9)$$

where $U_s(\zeta,t) = v_s$ at y=0. The solution of $U(\zeta,t)$ can be shown to be:

$$U(\zeta,t) = \frac{\rho}{\rho_c}\frac{E_c}{C(\zeta)}\left[1 - \frac{4K(\zeta)}{3 + 4\zeta^2}\right]\sqrt{\frac{D}{t}} \quad (10)$$

The displacement of the spray edge from the initial interface, y_{ca}, is computed by integrating $U(\zeta,t)$ with respect to time, and it follows that

$$y_{ca} = \frac{2\sqrt{Dt}}{C(\zeta)}\frac{\rho}{\rho_c}E_c \quad (11)$$

Eigenvalue of the Solution

The eigenvalue E_c is determined by substituting T, obtained from $\beta_T(\eta)$, and $U_s(\zeta,t)$, from Eqs. (2) and (10), into the equation of heat flux balance at the spray edge:

$$\lambda \left(\frac{\partial T}{\partial y} \right)_w = \left(Y_d [L + C_{pl}(T_w - T_s)] \right. \quad (12)$$
$$\left. + (1 - Y_d) C_{pg}(T_w - T_s) \right) \rho_c U_s(\zeta,t)$$

It follows that E_c can be computed from the characteristic equation:

$$\sqrt{\pi}\, E_c \exp(E^2_c) [1 + erf(E_c)] = B_c \quad (13)$$

where B_c is the mass transfer number of the spray analogous to single drop combustion theory and is defined as:

$$B_c \equiv \frac{[C_p(T_\infty - T_w) + q^o Y_{O\infty}/W_O \upsilon'_O]}{Y_d [L + C_{pl}(T_w - T_s)] + (1 - Y_d) C_{pg}(T_w - T_s)} \quad (14)$$

where $Y_d \equiv 4\pi a^3_o n_o \rho_l / 3\rho_c$ and $\rho_c \equiv 4/3\pi a^3_o n_o \rho_l + (1 - 4/3\pi a^3_o n_o)\rho_g$, for the droplet mass fraction and spray density respectively.

Spray Edge Temperature

The unknown spray edge temperature T_w, in Eq. (14), is determined from the Clausius-Claperon equation:

$$Y_{Fw} = \frac{W_F}{W_w} \exp\left[\frac{L W_F}{R} \left(\frac{1}{T_b} - \frac{1}{T_w} \right) \right] \quad (15)$$

where the Y_{iw} (i = F,I,P) are governed by the equations of species flux balance:

$$\rho C(\zeta) E_c \sqrt{\frac{D}{t}}\, Y_{iw} - \rho D \left(\frac{\partial Y_i}{\partial y} \right)_w = \rho_c U_s(\zeta,t)\, \Omega_i \quad (16)$$

Here, $\Omega_F = Y_d$, $\Omega_I = 1 - Y_d$, and $\Omega_P = 0$, are assigned, based on the assumption that the spray interior only contains inert gas and fuel droplets. Expressions for Y_i are obtained from the definitions of $\beta_i(\eta)$ and Eq. (7). By substituting Y_{iw} into Eq. (16), T_w is then computed by numerical iteration, and once T_w is known all the aforementioned variables are also determined.

Flamelet Diffusion Layer Structure

The distribution of fuel species in the neighbourhood of the spray flamelets is shown to be: $Y_F = 0$ for $\eta \geq \eta_f$ and

$$\frac{Y_F}{Y_{O\infty}} = \frac{\phi_w}{S} - \left(\frac{\phi_w}{S} + \frac{1}{S} \right) \frac{erf(\frac{\eta}{2} - E_c) + erf(E_c)}{1 + erf(E_c)} \quad (\eta < \eta_f) \quad (17)$$

where $\phi_w \equiv S Y_{Fw}/Y_{O\infty}$ and $S \equiv W_O \upsilon'_O / W_F \upsilon'_F$ represent the background equivalence ratio and the flame stoichiometry, respectively. The distributions of oxidizer and combustion products can also be found (not shown here) by the same procedures.

Figure 3 shows the variation of the mass fractions of fuel, oxidizer, and combustion products near an octane spray/air flamelet with a spray droplet mass fraction $Y_d = 25\%$ at different locations in the vortex field as characterized by the value of $\zeta = \Gamma t / 2\pi r^2$. The solid curve stands for $\zeta = 0$, dashed for $\zeta = 1$, dotted for $\zeta = 2$, and dash dotted for $\zeta = 3$. This plot shows the similarity between these different flamelets, and the time-dependent displacement of their locations, that is the value of $y_f / \sqrt{Dt}$ where $Y_F = Y_O = 0$.

Local Flamelet Motion

The flamelet location is determined by setting $\eta = C(\zeta) y_f / \sqrt{Dt}$ and $Y_F = 0$ in Eq. (17) and then

$$Y_f = \frac{2\sqrt{Dt}}{C(\zeta)} \left[E_c + erf^{-1} \left(\frac{\phi_w - erf(E_c)}{\phi_w + 1} \right) \right]$$
$$\equiv \frac{2\sqrt{Dt}}{C(\zeta)} (E_c + B_f) \quad (18)$$

The absolute flamelet displacement with respect to the initial interface, y_{fa}, can be shown to be:

$$y_{fa} = \frac{2\sqrt{Dt}}{C(\zeta)} \left[\left(1 - \frac{\rho}{\rho_c}\right) E_c + B_f \right] \quad (19)$$

The volumetric fuel consumption rate at the flamelet surface can be written as:

$$(\dot{J}''_F)_f = C(\zeta)\, Y_{O\infty} \sqrt{\frac{D}{t}} \left(\frac{E_c}{B_c} \right) \left(\frac{\phi_w + 1}{S} \right) \exp$$
$$\left(E^2_c - B^2_f \right) \equiv J_s\, C(\zeta) \sqrt{\frac{D}{t}} \quad (20)$$

It can be shown that the flamelet will be displaced toward the oxidizer when the fuel concentration exceeds the stoichiometric proportions ($\phi_w > 1$), as is usually the case for a diffusively burning dense fuel spray.

GLOBAL PROPERTY OF THE FLAME/VORTEX INTERACTION

Contours of the Vortex - Distorted Flame

The global flame contour is obtained by patching moving flamelet solutions for different values of ζ together. As a basis for patching, an isolated element of the interface contour is shown in Fig. 4. It can be shown that the polar coordinates of the neighbouring points, *f* and *e*, corresponding to the flamelet location and the spray edge are given by:

$$(r_f, \theta_f) = (r \pm y_{fa} \cos\psi, \theta \pm y_{fa} \sin\psi / r_f)$$

$$(r_e, \theta_e) = (r \mp y_{ea} \cos\psi, \theta \mp y_{ea} \sin\psi / r_e) \quad (21)$$

where $\psi = \tan^{-1}(1/2\zeta)$, and y_{ea} and y_{fa} are given by Eqs. (11) and (19), respectively. The "±" signs stand for a flamelet initially located on the RHS ($\theta = \zeta$) or the LHS ($\theta = \pi + \zeta$) of the vortex center respectively, and the "∓" signs refer to elements of the spray edge. Based on these relations, contours of the flame and the spray edge can then be drawn.

Figure 5 illustrates such contours for an octane spray/air diffusion flame in the field of a potential non-decaying vortex. The solid and dotted curves represent the flame contour and the spray edge contour respectively, and the void core indicates the region where vortex decay is significant for the same value of $\Gamma / 2\pi D$. The radius r_υ of this core is obtained by setting $\exp(-r^2/4\upsilon t) = 0.01$ in the expression for the velocity of a decaying vortex: $\upsilon_\theta = (\Gamma / 2\pi r)[1 - \exp(-r^2/4\upsilon t)]$. It can be seen that the spray flame lies totally outside this region, indicating the applicability of the present inviscid results to flame-vortex interaction problems. The space between contours of the flame and the spray edge contains

unburned fuel vapor, combustion products, and inert gas, while the central core may contain some unburned ed spray. It can be seen that the two branches of the flame shown in Fig. 1(b) are now deformed into a hook-like single flame with the hook tip being denoted as a critical point of the flame contour, (r^*_f,θ^*_f). In computing the flame contour, the restriction of $y_{fa}/r^*_f << 1$ has to be satisfied for the local flamelet flow analysis and patching procedures to remain valid.

Figure 6 demonstrates the validity of the potential approximations to a viscous decaying vortex case and shows the similarity between flame contours with different $\Gamma/2\pi D$. Plots (a) and (b) show that when the vortex Reynolds number $\Gamma/2\pi\upsilon$ is increased, the vortex-generated expanding and distorting effect on the flame is enhanced while the spray engulfment phenomenon also becomes more significant. Plots (a) and (c) indicate the minor change induced by an increase in spray droplet mass fraction, in the dense spray regime $0.2446 \le Y_d \le 0.7222$ for an octane spray. Plots (b) and (d) show the enlargement of the viscous core when the vortex Schmidt number υ / D is increased.

Spray Engulfment and the Reacted Core

The critical point of the flame contour is determined by simultaneously solving the relations $r_{fR} = r_{fL} = r^*_f$ and $\theta_{fR} = \theta_{fL} = \theta^*_f$. The Newton-Raphson method was used to solve the resultant equations. Since r^*_f is the radial position of the critical point of the flame contour, it is then used as the radius of the flame-bounded reacted core inside which combustion is no longer possible. However, as is evident from Fig. 5 this reacted core does not consist entirely of combustion products but also includes fuel vapor, inert gas, and unburned spray engulfed by the strong circulation of the vortex.

Figure 7 shows the results of the computation of r^*_f for different values of $\Gamma/2\pi D$. Based on these results, the following correlation was obtained:

$$r^*_f \approx K_3 (\Gamma/2\pi D)^{1/3} D^{1/2} t^{1/2} \tag{22}$$

The proportionality constant K_3 is slightly different for different values of Y_d since a larger Y_d leads to a larger flamelet displacement, resulting in an outward shift of the critical point.

Augmentation in Fuel Consumption Rate

The augmentation in fuel consumption rate (AFCR) is computed from an integral of the flamelet fuel flux rate, Eq. (20), along the flame contour and then subtracting the counterpart for the case without the vortex from the integration result. It has been shown that AFCR can be computed from the integral:

$$AFCR = \sum_i \int_{r^*_i}^{\infty} J_s \sqrt{\frac{D}{t}} \left[\Lambda(\zeta_i) \sqrt{1 + 4\zeta^2_i} \left(1 \pm \cos\psi_i \cos 2\psi_i \frac{y_{f_i}}{r_i}\right) - 1 \right] dr_i \tag{23}$$

where i=R and L for flame contours initially to the right and left of the vortex; the signs "±" are for i=R and L, respectively; and J_s is defined in Eq. (20).

The AFCR determined from Eq. (23) is shown[11] to be given by:

$$AFCR = J_s \sqrt{\Gamma D/2\pi} \left[2\sqrt{3} \left(\sqrt{\zeta^*_R} + \sqrt{\zeta^*_L} \right) - 6.4543 + O(\zeta^{*-1/2}_R) + O(\zeta^{*-1/2}_L) \right] + 2J_s D \left[(1-\rho/\rho_c) E_c + B_f \right] \left[(\zeta^*_R - \zeta^*_L) + (\psi^*_R - \psi^*_L) \right] \tag{24}$$

where ζ^*_R and ζ^*_L are obtained numerically in solving for r^*_f.

Figure 8 shows plots of AFCR for $5{,}730 \le \Gamma/2\pi D \le 10{,}185$ with Y_d=25%, 50%, and 70%. According to these plots, the following correlation is obtained:

$$\frac{AFCR}{J_s D} \approx K_4 (\Gamma/2\pi D)^{2/3} \tag{25}$$

where K_4 is weakly dependent on ϕ_w.

CONCLUSIONS

The time-dependent contour of a dense spray diffusion flame in the field of an incompressible plane potential vortex has been determined, based on the local flamelet displacement y_{fa}, obtained from a spray flamelet analysis. Similarity between flame contours for different values of $\Gamma/2\pi D$ is observed for a given fuel spray and oxidizer combination. A spray-engulfed reacted core bounded by the flame contour is identified with the radius r^*_f, which is the radial coordinate of the critical point of the flame contour. It is shown that with increasing $\Gamma/2\pi D$, the global flame contour will be expanded and distorted and the dimensionless radius $r^*_f/\sqrt{Dt}$ of the reacted core is found to increase. It is further shown that $r^*_f/\sqrt{Dt}$ is linearly proportional to $(\Gamma/2\pi D)^{1/3}$. The augmentation in volumetric fuel consumption rate of the interaction field is shown to be independent of time and linearly proportional to $(\Gamma/2\pi D)^{2/3}$. The present results can be considered as a good approximation for a viscous vortex with the same $\Gamma/2\pi D$, provided that $\Gamma/2\pi D$ is sufficiently large so that the restriction: $y_{fa}/r^*_f << 1$ is satisfied. While the above analysis involves many approximations, the roles of some of key parameters governing the vortex-spray interaction are identified.

NOMENCLATURE

Alphabatic

D	Binary diffusivity of species.
E_c	Eigenvalue, governed by Eq. (13).
h^o	Enthalpy of formation of species.
q^o	Heat of reaction of flame.
R_e	Vortex Reynolds number, defined as $\Gamma/2\pi\upsilon$.
r	Radial position, from the vortex center.
S	Flame stoichiometric coefficient, defined as $W_o\upsilon'_o/W_F\upsilon'_F$.
S_c	Vortex Schmidt number, defined as υ/D.
T	Temperature.
t	Time.
U	Spray vaporization wave speed.
u	x-component of velocity in flamelet flow.
v	y-component of velocity in flamelet flow.
W	Molecular weight.
x	Local coordinate aligned with flamelets.
Y	Species mass fraction.
Y_d	Droplet mass fraction in a spray.
y	Local coordinate normal to flamelets.
Γ	Vortex circulation.
ε	Vortex-generated local flow strain rate.

ζ	Parameter, defined as $\Gamma t/2\pi r^2$.
η	Similarity variable, defined as $y/\sqrt{Dt}$.
θ	Angular coordinate.
λ	Thermal conductivity.
υ	Stoichiometric coefficients.
ρ	Density.
ϕ_w	Background equivalence ratio, $\phi_w \equiv SY_{I,w}/Yo_\infty$.
ψ	Angle between flamelet and v_θ, $\tan\psi = 1/2\zeta$.

Subscripts

a	Absolute coordinate.
f	Flame.
g	Spray vapor phase.
F,O,P	Fuel, oxidizer and combustion products.
l	Spray droplet phase.
o	Initial condition.
s	Spray or Saturation conditions.
w	Spray edge.
∞	Condition outside of flamelet diffusion layer.

Superscripts

*	Critical point of flame contours.

REFERENCES

1. Marble, F.E., *Recent Advances in the Aerospace Sciences* (C.Casci, Ed.), Plenum Press, New York and London, pp. 395-413, 1985.
2. Karagozian, A.R., and Marble, F.E., Comb. Sci. and Tech. **45**, 65, (1986).
3. Karagozian, A.R., and Manda, B.V.S., Comb. Sci. and Tech. **49**, 185, (1986).
4. Laverdant, A.M., and Candel, S.M., Comb. Sci. and Tech. **60**, 79, (1988).
5. Manda, B.V.S., and Karagozian, A.R., Comb. Sci. and Tech. **61**, 101, (1988).
6. Rehm, R.G., Baum, H.R., Lozier, D.W., and Aronson, J., Comb. Sci. and Tech. **66**, 293, (1989).
7. Cetegen, B.M., and Sirignano, W.A., Comb. Sci. and Tech. **72**, 157, (1990).
8. Shiah, S.M., and Sichel, M., Spring Technical Meeting/Central State Section, distributed copy, The Combustion Institute, Nashville, Tennessee, April 1991.
9. Sichel, M., and Palaniswamy, S., Twentieth Symposium (International) on Combustion, p. 1789, The Combustion Institute, 1984.
10. Williams, F.A., Combustion Theory, 2nd Ed., Benjamin/Cummings Publishing Inc., 1985.
11. Shiah, S.M., Dynamic Behavior of a Dense Spray Diffusion Flame in a Potential Vortex Structure, Ph.D. Thesis, Dept. of Aerospace Engineering, The University of Michigan, December 1991.

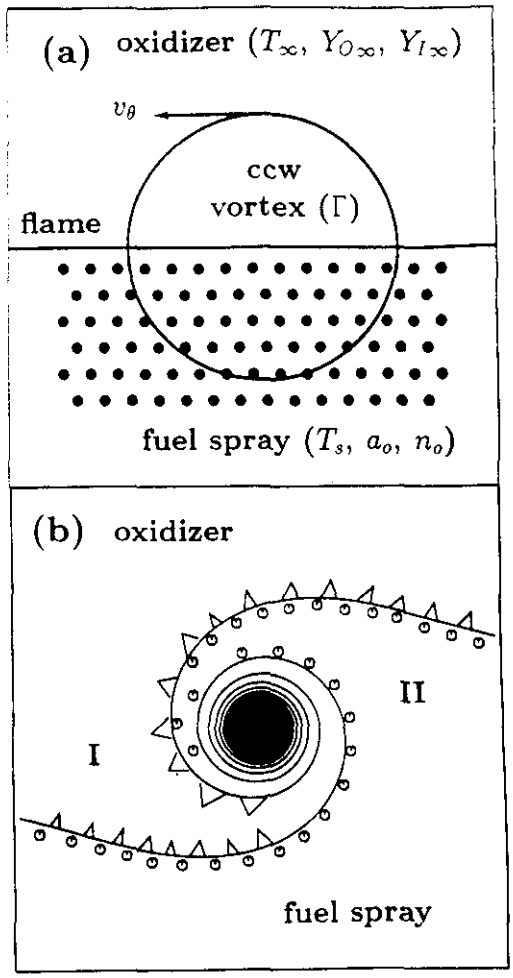

Fig. 1: (a) Initial configuration of the spray diffusion flame/vortex interaction; (b) Incipient relative motion of the spray diffusion flame and the edge of the spray (*solid:* contour of the initial spray diffusion flame; *arrowheads:* motion of the spray flamelets; *dots:* motion of the spray edge).

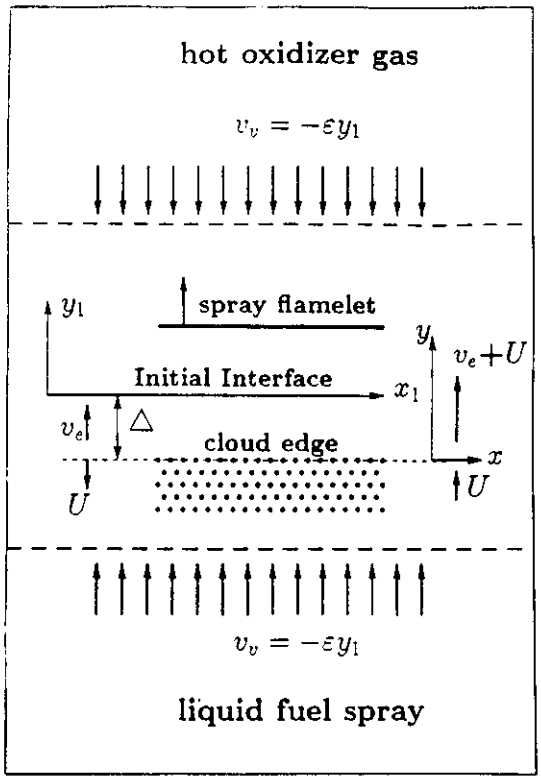

Fig. 2: Local spray flamelet configuration for the spray diffusion flame/vortex interaction.

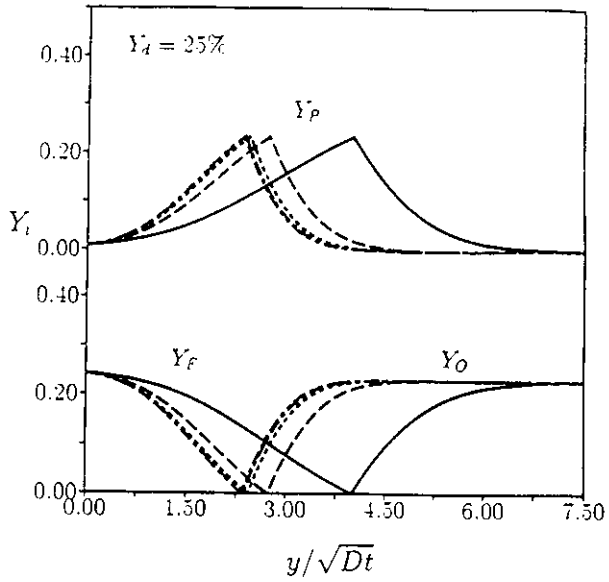

Fig. 3: Flow-strained local diffusion layer structure of spray flamelets in the field of a non-decaying potential vortex (*solid:* ζ=0 and for flamelets in the far field away from the vortex; *dashed:* ζ=1; *dotted:* ζ=2; *dash dotted:* ζ=3; and *dot dotted:* ζ=4; where $\zeta \geq 3$ represents flamelets in the neighbourhood of the vortex center).

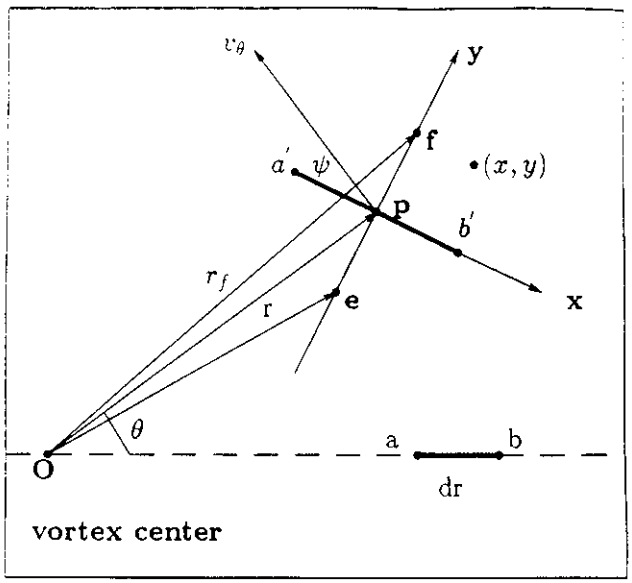

Fig. 4: Geometric relations between the local spray flamelet configuration and the global vortex configuration, after some time has elapsed (a'b': the initial interface of the spray and the oxidizer; *f*: location of the spray flamelet; and e: location of the spray edge element).

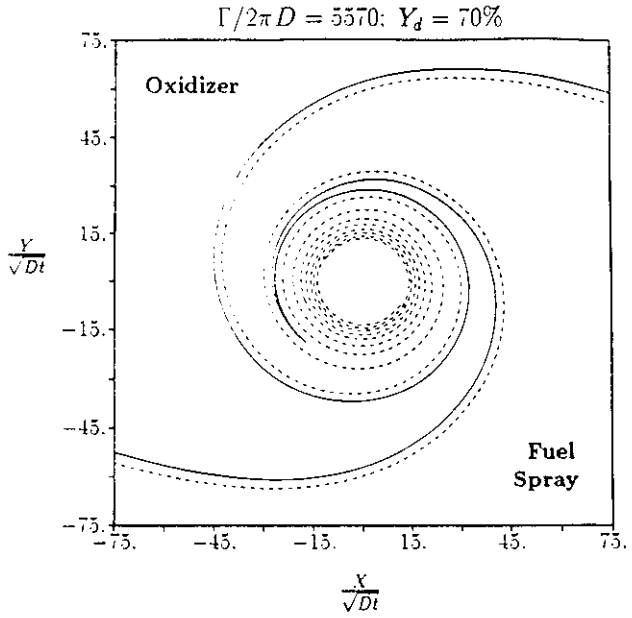

Fig. 5: Contours of a typical octane spray-air diffusion flame (Y_d=70%) in the field of a non-decaying potential vortex with $\Gamma/2\pi$D=5570 (*solid:* contour of the spray diffusion flame; *dotted:* contour of the spray edge).

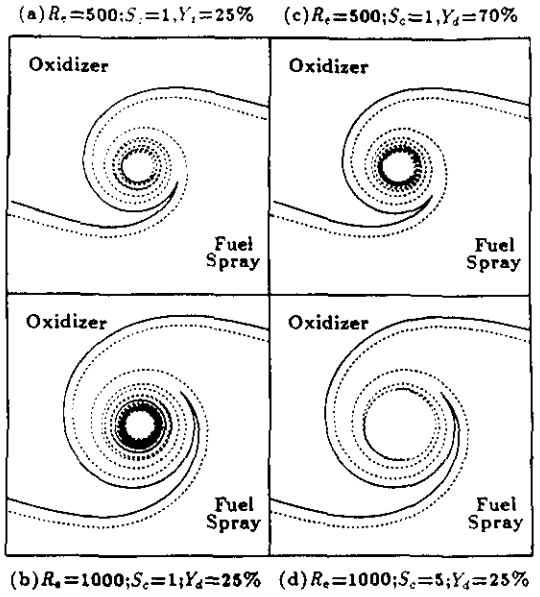

Fig. 6: Approximations for the cases of interaction between an octane/air spray diffusion flame and a viscous decaying vortex, under the conditions of: (a) R_c=500; S_c=1.0; Y_d=25%, (b) R_c=1000; S_c=1.0; Y_d=25%, (c) R_c=500; S_c=1.0; Y_d=70%, (d) R_c=1000; S_c=5.0; Y_d=25% (*solid:* contours of the spray diffusion flame; *dotted:* contours of the spray edge; *core:* viscous core of the vortex; equal scale for each plot with span: $X/\sqrt{Dt}$=-35 to 35 and $Y/\sqrt{Dt}$=-35 to 35).

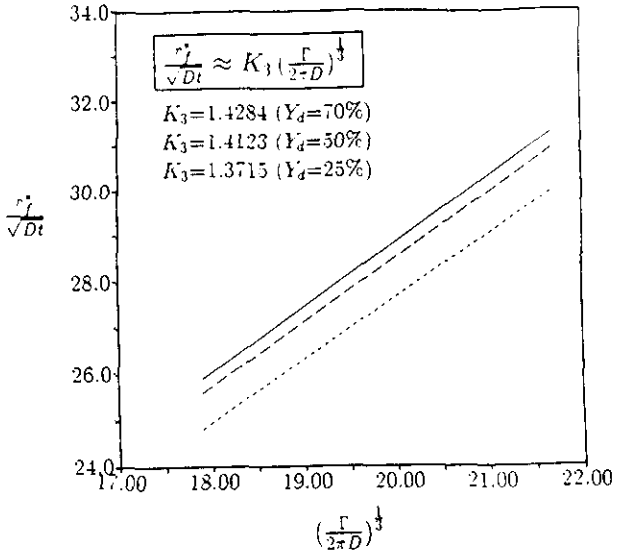

Fig. 7: Variation of the reacted core radius of the interaction field of a dense spray diffusion flame and a non-decaying potential vortex with $\Gamma/2\pi D$ (*solid:* Y_d=70%; *dashed:* Y_d=50%; *dotted:* Y_d=25%).

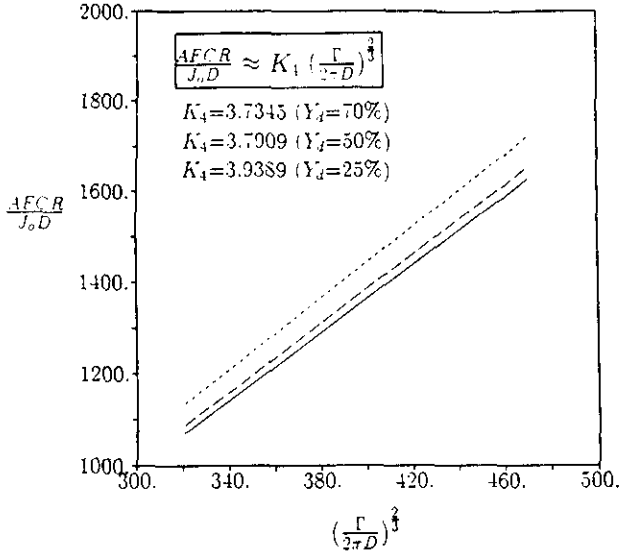

Fig. 8: Variation of the augmentation of the global fuel consumption rate due to the interaction of a dense spray diffusion flame and a non-decaying potential vortex with $\Gamma/2\pi D$ (*solid:* Y_d=70%; *dashed:* Y_d=50%; *dotted:* Y_d=25%).